Fluorochrome-labeled monoclonal antibody with characteristic M-shaped spectral peak for optical imaging: Dual-labeling versus mixture of fluorochromes

Jan Menke*, Thomas Kruewel, and Christian Dullin

Institute for Diagnostic and Interventional Radiology, University Medical Center, Georg August University, 37075 Goettingen, Germany

**Corresponding author: Menke-J@T-Online.de*

Received October 15, 2014; accepted March 26, 2015; posted online May 4, 2015

In this work two different fluorochromes (Alexa 594 and Alexa 680) are conjugated to the same monoclonal antibody (Cetuximab) for obtaining a characteristic M-shaped dual-peak spectrum. Dual-labeling of Cetuximab by mixing both fluorochromes before the conjugation step gives spectral results similar to those of mixing of fluorochrome-labeled Cetuximab after the conjugation step ($P > 0.05$). In conclusion, both methods may be used equivalently for producing a dual-labeled single-antibody probe. Future studies may test whether the M-shaped spectrum may increase the diagnostic confidence in tumor-targeted multispectral optical imaging.

OCIS codes: 170.0170, 170.3880, 170.4580.

doi: 10.3788/COL201513.051701.

Optical imaging is useful in preclinical research and already has clinical and research applications in humans, such as fluorescence-guided sentinel node biopsy, diffuse optical breast tomography, and photoacoustic breast imaging, and further refinements are ongoing[1–6]. It represents a method for molecular imaging, particularly when using exogenous optical reporters. Fluorochrome-labeled monoclonal antibodies are applied in preclinical optical cancer imaging and are promising for clinical translation[7]. An example is fluorochrome-labeled cetuximab that is targeted against the epidermal growth factor receptor (EGFR)[8]. The same antibody could potentially be used for immunotherapy[9–11], while additional optical imaging could assess whether and when the antibody is concentrated in the tumor. Dual-labeling or multicolor labeling of monoclonal antibodies has previously been performed for simultaneously aiming at different targets[7,12–16]. However, simultaneously aiming with two different fluorochromes at exactly the same target has not been studied so far in optical imaging. Particularly in case of high heterogeneous background signals or imaging artifacts the diagnostic confidence of future preclinical or clinical macroscopic optical imaging at depths ≥5–10 cm with tumor-targeted probes could possibly be increased, if two different characteristic spectral peaks must be detected at the same image position. This work's aim was to label a single monoclonal antibody with two different fluorochromes for obtaining characteristic M-shaped absorption/emission spectra, and study whether mixing the fluorochromes before or after the conjugation step makes any difference. The dual-color monoclonal antibodies were produced and were studied successfully, and the results are discussed in context with the literature.

Regarding probes, the fluorochromes Alexa Fluor 594 and 680 (Life Technologies, Frankfurt, Germany) were used in this work. They were chosen since their combined absorption/emission spectra results in the planed M-shaped dual-peak spectrum. In principle, fluorochromes from other companies or with other spectral characteristics could have been used alternatively. Four different fluorochrome-labeled monoclonal antibody probes were generated (Table 1), using the monoclonal anti-EGFR antibody Cetuximab (Erbitux, Merck, Darmstadt, Germany) and reactive dyes from Alexa Fluor protein labeling kits.

Regarding Probe A594, according to the product's labeling protocol Cetuximab (5_mg/mL) was diluted with phosphate-buffered saline (PBS) to 2 mg/mL, and 0.5 mL of this solution [1 mg immunoglobulin G (IgG)] was added to one vial of Alexa Fluor 594. The reaction mixture was stirred at slow speed on a magnetic stirrer for 1 h at room temperature. Afterwards, the fluorochrome-conjugated antibodies were purified by three centrifugal filtering cycles, using filters with 10 kDa cutoff (Amicon Ultra, 0.5 mL centrifugal filters, Merck Millipore Ltd., Carrigtwohill, Ireland) and a benchtop centrifuge (Centrifuge 5424, Eppendorf AG, Hamburg, Germany) for 8 min at 14600 revolutions/min. After each filtering the permeate was removed and the dye-labeled antibody retentate was refilled with an equal volume of PBS solution.

Regarding Probe B680, in Probe B680 the same was done with Alexa Fluor 680.

Regarding Probe C594/680, a total of 2 mg Cetuximab (1 mL of the IgG-PBS solution described previously) was added to one vial of Alexa Fluor 598 plus one vial of Alexa 680, and the subsequent antibody labeling was performed

Table 1. Fluorochrome-Labeled Monoclonal Antibody Probes

Probe	Absorption Peak(s) (nm)	Emission Peak(s) (nm)	Cetuximab (Erbitux)	Alexa Fluor 594	Alexa Fluor 680
A594	590	617	1 mg	One vial	—
B680	679	702	1 mg	—	One vial
C594/680	590 + 679	617 + 702	2 mg	One vial	One vial
D594 + 680	590 + 679	617 + 702	Mix equal volumes of Probes A + B		

with this fluorochrome mixture. This represents mixing the fluorochromes before the antibody-conjugation step.

Regarding Probe D594 + 680, equal volumes of Probes A594 and B680 were mixed to obtain Probe D594 + 680. This represents mixing the fluorochromes after the antibody-conjugation step.

Regarding optical fluorescence measurements, the four probes were diluted with PBS to concentrations of 100, 50, 25, and 12.5 mg IgG/mL. The resulting 16 samples (four probes × four dilutions) were filled in a 48-well-plate (6 × 8 wells having 10 mm diameter). The samples' fluorescence emission spectra were measured by an IVIS Spectrum optical imaging system (PerkinElmer, Waltham, MA) in the epifluorescence mode. Per sample this was done by a total of 94 suitable combinations of 30 nm width bandpass excitation filters (440–760 nm) and 20 nm width bandpass emission filters (510–850 nm) to obtain 94 different multispectral two-dimensional excitation/emission measurements. In the images the samples' fluorescence intensity was quantified as average radiant efficiency in units of photons/second/square centimeter/radiant per milliwatt/square centimeter after placing regions-of-interest at the wells. The reproducibility of these measurements was assessed by five repeated optical measurements of the 100 mg IgG/mL Probes A594 and B680 at their spectral peaks, and was expressed as coefficient of variation (standard deviation/mean).

Regarding spectral and statistical analysis, per sample the 94 acquired multispectral data were plotted with the emission wavelength on the horizontal x-axis and the fluorescence intensity on the vertical y-axis. The enfolding curve of maximum intensity values resembles characteristics of the true emission spectrum, but is not identical to it. Therefore optical measurements of the pure Probes A594 and B680 served for reference in this work, when assessing the spectral characteristics of Probe C594/680 (fluorochromes mixed before conjugation) and Probe D594 + 680(mixed after antibody conjugation). Additionally, the average radiant efficiencies of Probe C594/680 and Probe D594 + 680 were compared by regression analysis on a logarithmic scale, using PROC REG from SAS 9.3 (SAS Institute, Cary, NC) with a significance level of $P < 0.05$. The TEST statement was used to test whether the corresponding intercept was zero and the slope was one, which would indicate similarity of both probes' fluorescence spectra.

Probes A594 and B680 generated their expected single-peak emission spectra [Figs. 1(a) and 1(b)]. Probe D594 + 680 showed an M-shaped dual spectral peak, expected from mixing Probes A594 and B680 [Fig. 1(d)]. Compared to the spectral peaks of the pure Probes A594 and B680 the peaks of the M-shaped spectrum do have half the magnitude, but the total fluorescence signal (area under the curve) is comparable. The spectral shape of Probe C594/680 [Fig. 1(c)] was nearly similar to Probe D594 + 680.

In each panel of Fig. 1 the probes' fluorescence intensity is given as average radiant efficiency in units of photons/second/square centimeter/radiant per milliwatt/square centimeter on the vertical axis. The horizontal axis shows the emission wavelength (nanometers). The corresponding excitation wavelengths (nanometers) of the multispectral fluorescence measurements are presented in different colors. In total, 94 excitation–emission filter combinations were measured per probe. The enfolding gray curves resemble the true fluorescence emission spectra, but are not identical to them. Therefore the pure probes [Figs. 1(a) and 1(b)] are shown for reference, when assessing Figs. 1(c) and 1(d). The peak fluorescence intensity was 2.24×10^9 units in Probe A594 [Fig. 1(a)] and 1.78×10^9 units in Probe B680 [Fig. 1(b)]. In these probes one vial reactive dye had been used for labeling 1_mg Cetuximab (Table 1). In Probe D594 + 680 [Fig. 1(d)] both peaks of the M-shape had only half that signal intensities, since in this probe effectively 1/2 vial of Alexa 594 and 1/2 vial of Alexa 680 had been used for labeling 1_mg Cetuximab (Table 1). However, the total fluorescence signal (area under the curve) was comparable, since Probe D594 + 680 has two peaks instead of one peak. The same applies to Probe C594/680.

In the regression analysis the average radiant efficiencies of Probe C594/680 were also nearly similar to Probe D594 + 680 ($P > 0.05$). The data of this regression analysis are presented in Fig. 2.

In Fig. 2 the fluorescence intensities are given on a logarithmic scale as average radiant efficiency in units of photons/second/square centimeter/radiant per milliwatt/square centimeter. The diagonal line is the line-of-identity. In the regression analysis the multispectral fluorescence intensities of Probe C594/680 (dual-labeling before conjugation) were nearly similar to Probe D594 + 680 (mixing of Probes A594 and B680 after conjugation). In the model

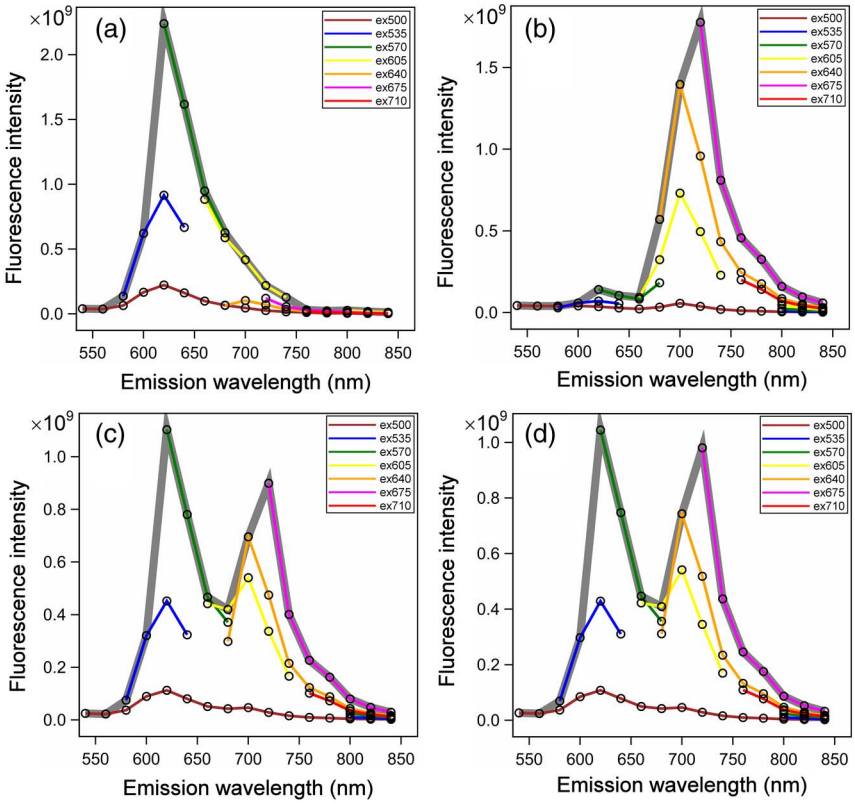

Fig. 1. Multispectral fluorescence emission measurements.

equation log(C594/680) = intercept + slope × log(D594+680) the intercept of −0.032 [95% confidence interval (CI): −0.078 to 0.015] was not significantly different from zero ($P = 0.18$) and the slope of 1.003 (95% CI: 0.996–1.009) was not significantly different from one ($P = 0.35$), indicating no major difference between the emission spectra of both probes.

These results were obtained for 100 mg IgG/mL. Comparable results were also obtained for the other probe concentrations of 50, 25, and 12.5 mg IgG/mL. The coefficient of variation of the average peak radiant efficiencies was 1.4% for Probe A594 (excitation bandpath filter 555–585 nm, emission bandpass filter 610–630 nm) and 1.2% for Probe B680 (excitation bandpath filter 660–690 nm, emission bandpass filter 710–730 nm), indicating high reproducibility of the fluorescence measurements.

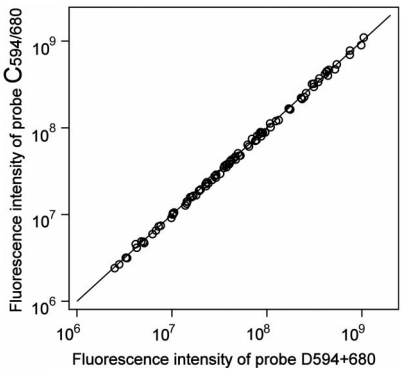

Fig. 2. Fluorescence intensity of Probe C594/680 versus Probe D594 + 680.

Dual-labeling of monoclonal antibodies and other molecular carriers is used for example in multi-modality molecular imaging, such as correlation of optical imaging with nuclear imaging[7,12] or with magnetic resonance imaging[16]. Also, dual-color or multicolor imaging with fluorochromes is used for depicting different targets within the same image[13–15]. In this work a concept is presented for labeling the same monoclonal antibody with two different fluorochromes. The result is a characteristic M-shaped excitation and emission spectrum that originates from two overlapping spectral peaks.

In multispectral optical or optoacoustic tomography and other modalities with background signals or image reconstruction artifacts it may be studied whether this could increase the diagnostic confidence of tumor-targeted preclinical/clinical imaging, since two images of different wavelengths must then show local peaks to indicate presence of the fluorochrome-labeled monoclonal antibodies. The diagnostic information from both images could then for example be combined by a minimum intensity algorithm. A corresponding simulation study can be requested from the first author.

Particularly in tomographic optical measurements the signal intensities are depth-dependent due to the exponential decay of light intensity from the surface to the target. Therefore it may be difficult to apply an absolute signal intensity threshold for diagnosing a tumor (e.g., in large human organs such as the breast), and the

M-shaped spectral characteristic might then be useful as a nonquantitative spectral fingerprint in the diagnostic decision between presence or absence of a tumor, comparable to spectral analysis in magnetic resonance spectroscopy[17].

In this work it was equivalent, whether Cetuximab was dual-labeled with fluorochromes (Probe C594/680) or whether different single-color antibodies were mixed (Probe D594 + 680). In the dual-labeling method (Probe C594/680) variations in the labeling reaction affect both fluorochromes similarly, so that the molar ratio of both fluorochromes may be quite constant. In the mixing method (Probe D594 + 680) any differences between both single labeling reactions or slight inaccuracies in mixing the component volumes might result in varying molar ratios of both fluorochromes. Therefore the dual-labeling method might be preferred for having a well-defined reproducible spectral M-shape. On the other hand, the mixing method allows for more flexibility in the molar ratio of both antibody-conjugated fluorochromes, if desired.

Future *in vivo* research may show whether the presented M-shaped spectral peak of a dual-color monoclonal antibody is useful for identifying tumor-suspicious regions or for increasing the corresponding diagnostic confidence. For using the method a multi-spectral approach or at least a dual-spectral approach (at both spectral peaks of the two fluorochromes) is required to utilize the M-shaped absorption or emission pattern, which makes the signal detection more sophisticated than in traditional single-peak fluorescence imaging. The method could be applied in multispectral imaging, where tissue components and exogenous reporters can be differentiated by spectral unmixing[18–21]. Such multispectral imaging with spectral unmixing is possible for different modalities, such as near-infrared spectroscopy[22–24], fluorescence imaging (e.g., in the IVIS optical imaging system of this work), diffuse optical tomography[25,26], and multispectral optoacoustic tomography (MSOT)[27–30]. In optoacoustic and optical tomography the M-shaped extinction spectrum is utilized, whereas in fluorescence imaging the M-shaped emission spectrum is utilized. In many fluorochromes the spectral M-shape would be present both in the excitation spectrum and the emission spectrum according to the mirror-image rule in fluorescence[31]. In optical or optoacoustic preclinical/clinical research an additional fluorescence imaging could serve for multi-modal correlation, using the same M-shape spectral properties of the dual-color monoclonal antibodies.

In deep tissue the effective near-light absorption is spectrally dependent due to wavelength-dependent scattering and absorption, and this may cause a distorted M-shape when viewing the raw spectral data. This general challenge in multispectral imaging could be solved by spectral unmixing that is also required for identifying other tissue components[18–21].

If it is intended to apply a marker with a very characteristic spectral signature, then other markers might also be useful. For example, some kinds of up-conversion nanoparticles are able to emit fluorescence with multiple peaks[32,33]. This up-conversion can avoid the effects of autofluorescence. However, in deep-tissue near-infrared imaging the spectral range for any multicolor marker is limited, since the spectral window is confined to about 675–925 nm plus a smaller window around 1050 nm, and therefore the number of distinguishable spectral peaks is also limited.

This work was limited to investigating two fluorochromes with one type of antibody. Similar *in vitro* testing could be performed when using other fluorochromes or antibodies. This work was limited to presenting the concept of an M-shaped dual-peak spectrum and producing the required dual-labeled fluorochrome probes. Such probes could then be tested in different preclinical (and potentially clinical) settings with different optical imaging methods. It was beyond the aim of this work to perform such subsequent application studies. However, a simulation is provided that illustrates how a minimum intensity algorithm could be applied to utilize the method.

In conclusion, for producing a dual-color monoclonal antibody with the named materials it makes no difference whether mixing the fluorochromes before or after the antibody-conjugation step. The concept of a characteristic M-shaped absorption/emission spectrum could be evaluated in future antibody-based tumor-targeted optical imaging studies.

References

1. A. Taruttis and V. Ntziachristos, Am. J. Roentgenol. **199**, 263 (2012).
2. L. Xiong, E. Gazyakan, W. Yang, H. Engel, M. Hünerbein, U. Kneser, and C. Hirche, Eur. J. Surg. Oncol. **40**, 843 (2014).
3. D. R. Leff, O. J. Warren, L. C. Enfield, A. Gibson, T. Athanasiou, D. K. Patten, J. Hebden, G. Z. Yang, and A. Darzi, Breast. Cancer Res. Treat. **108**, 9 (2008).
4. G. Wang, H. Zhao, Q. Ren, and C. Li, Chin. Opt. Lett. **12**, 051703 (2014).
5. X. Li, J. Yang, X. Sheng, J. Zhang, D. Cui, Q. Peng, and Z. Xu, Chin. Opt. Lett. **11**, 111901 (2013).
6. W. Xie, Y. Liu, Z. Li, and H. Li, Chin. Opt. Lett. **12**, 051702 (2014).
7. S. Oliveira, R. Cohen, M. S. Walsum, G. A. van Dongen, S. G. Elias, P. J. van Diest, W. Mali, and P. M. van Bergen En Henegouwen, EJNMMI Res. **2**, 50 (2012).
8. S. Ke, X. Wen, M. Gurfinkel, C. Charnsangavej, S. Wallace, E. M. Sevick-Muraca, and C. Li, Cancer Res. **63**, 7870 (2003).
9. I. Zafir-Lavie, Y. Michaeli, and Y. Reiter, Oncogene **26**, 3714 (2007).
10. D. M. Goldenberg and R. M. Sharkey, Oncogene **26**, 3734 (2007).
11. K. Strebhardt and A. Ullrich, Nat. Rev. Cancer **8**, 473 (2008).
12. M. Ogawa, C. A. Regino, J. Seidel, M. V. Green, W. Xi, M. Williams, N. Kosaka, P. L. Choyke, and H. Kobayashi, Bioconjug. Chem. **20**, 2177 (2009).
13. J. J. Starling, N. A. Hinson, P. Marder, R. S. Maciak, B. C. Laguzza, J. R. Corvalan, and W. Smith, Cancer Res. **48**, 6211 (1988).
14. S. Wang, H. Kong, X. Gong, S. Zhang, and X. Zhang, Anal. Chem. **86**, 8261 (2014).
15. M. Bates, G. T. Dempsey, K. H. Chen, and X. Zhuang, ChemPhysChem **13**, 99 (2012).

16. Y. Liu, K. Ai, Q. Yuan, and L. Lu, Biomaterials **32**, 1185 (2011).
17. R. E. Lenkinski and M. D. Schnall, "MR spectroscopy and the biochemical basis of neurological disease," in *Magnetic Resonance Imaging of the Brain and Spine*, S. W. Altlas, ed. 2nd ed. (Lippincott–Raven, 1996), Chap. 2, pp. 1619–1653.
18. N. Keshava, Lincoln Lab. J. **14**, 55 (2003).
19. H. Xu and B. W. Rice, J. Biomed. Opt. **14**, 064011 (2009).
20. T. Pengo, A. Munoz-Barrutia, I. Zudaire, and C. Ortiz-de-Solorzano, PLoS ONE **8**, e78504 (2013).
21. J. Glatz, N. C. Deliolanis, A. Buehler, D. Razansky, and V. Ntziachristos, Opt. Express **19**, 3175 (2011).
22. J. Menke, U. Voss, G. Möller, and G. Jorch, Biol. Neonate **83**, 6 (2003).
23. J. Menke, H. Stöcker, and W. Sibrowski, Transfusion **44**, 414 (2004).
24. J. Menke and G. Möller, Pediatr. Cardiol. **35**, 155 (2014).
25. C. Li, H. Zhao, B. Anderson, and H. Jiang, Med. Phys. **33**, 627 (2006).
26. C. Li, S. R. Grobmyer, L. Chen, Q. Zhang, L. L. Fajardo, and H. Jiang, Appl. Opt. **46**, 8229 (2007).
27. D. Razansky, A. Buehler, and V. Ntziachristos, Nat. Protoc. **6**, 1121 (2011).
28. E. Herzog, A. Taruttis, N. Beziere, A. A. Lutich, D. Razansky, and V. Ntziachristos, Radiology **263**, 461 (2012).
29. D. Razansky, C. Vinegoni, and V. Ntziachristos, Opt. Lett. **32**, 2891 (2007).
30. D. Razansky, J. Baeten, and V. Ntziachristos, Med. Phys. **36**, 939 (2009).
31. J. R. Lakowicz, *Principles of Fluorescence Spectroscopy*, 3rd ed. (Springer, 2006) pp. 6–8, 13, 443–476.
32. Z. Li and Y. Zhang, Nanotechnology **19**, 345606 (2008).
33. F. Wang and X. Liu, J. Am. Chem. Soc. **130**, 5642 (2008).